

A Monolithic Photovoltaic-Photoelectrochemical Device for Hydrogen Production via Water Splitting

Oscar Khaselev and John A. Turner*

Direct water electrolysis was achieved with a novel, integrated, monolithic photoelectrochemical-photovoltaic design. This photoelectrochemical cell, which is voltage biased with an integrated photovoltaic device, splits water directly upon illumination; light is the only energy input. The hydrogen production efficiency of this system, based on the short-circuit current and the lower heating value of hydrogen, is 12.4 percent.

The direct photoelectrolysis of water at the semiconductor electrolyte interface is not only of scientific interest but also could produce benefits such as cost and energy savings over coupled photovoltaic (PV)-electrolysis systems for H_2 production (1). However, the lack of a stable, efficient light-absorption system coupled with suitable semiconductor-redox energetics has kept photoelectrochemists from reaching this goal.

Obstacles to direct photoelectrolysis of water are the lack of efficient light absorption (for reasonable solar efficiencies, the band gap must be less than 2.0 eV), corrosion of the semiconductor (thermodynamically, most useful semiconductors are photochemically unstable in water), and energetics (the difficulty of matching the semiconductor band-edge energies with the H_2 and O_2 evolution reactions) (2, 3). The most photochemically stable semiconductors in aqueous solution are oxides, but their band gaps are either too large for efficient light absorption or their semiconductor characteristics are poor (4). Semiconductors with better solid-state characteristics are typically thermodynamically unstable with respect to oxidation (2). However, *p*-type semiconductors generally offer some protection against photocorrosion, because under illumination the surface is cathodically protected. Heller (5, 6) has shown that *p*-type indium phosphide is stable in strong acid under illumination and H_2 evolution but requires an external bias for water splitting. In earlier work, we identified *p*-type gallium indium phosphide (*p*-GaInP₂) as perhaps a perfect semiconductor for water splitting. Although its band gap is in the ideal range (1.8 to 1.9 eV), the energetics of its band edges are not correct for water splitting, needing an additional 300-mV bias (7). Although it is possible to

move its band edges to some extent, their energetic positions are still inadequate to effect water splitting (8).

A number of approaches have been tried to overcome some of the obstacles to the direct splitting of water. Cells with two simultaneously illuminated semiconductors have been used (9–11). Multiple-junction amorphous silicon devices have also been reported by Sakai *et al.* (12) and Lin *et al.* (13). Augustynski *et al.* (14) have reported a water splitting system using a dye-sensitized nanocrystalline solar cell coupled to a tungsten trioxide electrode. However, each of their systems operated separately and they were not integrated into a monolithic device. Although all of these systems had some success, their efficiencies were rather low (<7%).

We now report a direct water electrolysis system based on a novel, integrated, monolithic photoelectrochemical (PEC)/PV device (Fig. 1A). This device is patterned after the GaInP₂/GaAs *p/n*, *p/n* tandem cell device grown at the National Renewable Energy Laboratory (15). The solid-state tandem cell consists of a GaAs bottom cell connected to a GaInP₂ top cell through a tunnel diode interconnect. The top *p/n* GaInP₂ junction, with a band gap of 1.83 eV, is designed to absorb the visible portion of the solar spectrum; and the bottom *p/n* GaAs junction, with a band gap of 1.42 eV, absorbs the near-infrared portion of the spectrum transmitted through the top junction. Although single-gap electrodes have a solar conversion efficiency limit of 32%, tandem-junction devices have an efficiency limit of 42% (16). The maximum theoretical solar-to-electrical efficiency for the present combination of band gaps is about 34% (17). Our device differs from the standard solid-state tandem cell in that a PEC Schottky-type junction has replaced the top *p/n* junction. This device then is a PEC device that is voltage-biased with an integrated PV device. Under illumination, electrons flow toward the illuminated surface and holes flow toward the ohmic contact.

Water is split directly upon illumination, light being the only energy input.

The *p*-GaInP₂/GaAs cells used in this study were grown by atmospheric-pressure organometallic vapor-phase epitaxy. Details of material growth and cell processing have been previously reported (18). The cell structure consists of a top layer of epitaxially grown *p*-Ga_{0.52}In_{0.48}P (abbreviated as *p*-GaInP₂) 4.0 ± 0.5 μm thick, connected in series via a low-resistivity, grown-in tunnel junction (TJ) to a GaAs *p/n* bottom cell on a GaAs substrate. The photoelectrochemical characteristics of the present cell were compared with those of a similarly grown *p*-GaInP₂ epilayer on a GaAs substrate. We have studied a number of similar devices with varying thicknesses of the top layer (19). The present configuration produced the best overall results and is reported here.

Standard chemical and electrochemical procedures were used (20), with the surface of the samples being coated with a platinum catalyst (21). Illumination for the photoelectrolysis was produced by a fiber optic illuminator with a 150-W tungsten-halogen lamp. To measure the light irradiance on the surface of the sample, a calibrated PV tandem cell was mounted into the electrode holder inside the cell in the manner similar

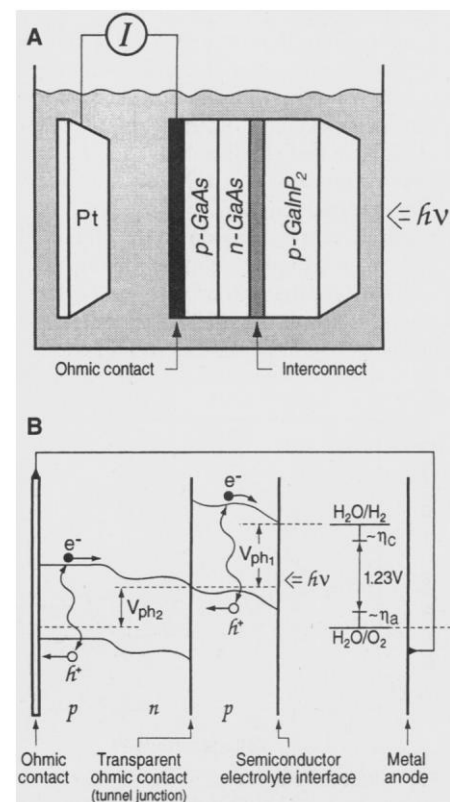


Fig 1. (A) Schematic of the monolithic PEC/PV device. (B) Idealized energy level diagram for the monolithic PEC/PV photoelectrolysis device.

National Renewable Energy Laboratory, 1617 Cole Boulevard, Golden, CO 80401-3393, USA.

*To whom correspondence should be addressed. E-mail: jturner@nrel.gov

to that used for the photoelectrodes. The measured light irradiance was 1.19 ± 0.05 W/cm²: about 11 suns (22).

For the PEC/PV configuration to work properly, the GaAs bottom cell must provide sufficient voltage to overcome any energetic mismatch between the band edges of the GaInP₂ and the water redox reactions, and must also provide any additional voltage needed to overcome overvoltage losses from the H₂ and O₂ evolution reactions. The total photovoltage output must include the thermodynamics for water splitting (1.23 V); polarization losses η_a and η_c for the anodic and cathodic processes, respectively; and the current-resistance potential drop in the bulk of the electrolyte, which can be significant when gas evolution occurs. An idealized energy-level diagram for the photolytic splitting of water with this device (Fig. 1B) illustrates the process, which includes two photons and one separated electron-hole pair. Light incident on the PEC/PV configuration first enters the wide band gap *p*-GaInP₂ layer, in which the more energetic photons are absorbed, resulting in electron-hole pair excitation and producing photovoltage V_{ph1} . Less energetic photons penetrate through the GaInP₂ and are absorbed by a GaAs bottom *p/n* junction generating photovoltage V_{ph2} . One set of holes and electrons are recombined at the tunnel junction. If the resultant photovoltage $V_{ph} = V_{ph1} + V_{ph2}$ is greater than that required for photoelectrolysis for this particular cell configuration, it will drive the water reduction reaction at the semiconductor electrode and water oxidation at the counterelectrode. Two photons are required to produce one electron in the external circuit, so four photons are required to produce one molecule of H₂. This is an example of a D4 scheme (16).

This configuration can easily be designed to do oxidation as well as reduction at the semiconductor-electrolyte interface.

For water-splitting reactions, however, H₂ production at the surface of the semiconductor is preferred for two reasons: (i) the H₂ evolution reaction has the lowest overvoltage losses, so the requirement for a catalyst is less, thus allowing an optimized counterelectrode to be used for the more complex O₂ evolution reaction; and (ii) under illumination, the semiconductor surface is cathodically protected.

Figure 2 shows photocurrent-voltage curves for platinum-catalyzed *p*-GaInP₂(Pt) and *p*-GaInP₂(Pt)/TJ/GaAs electrodes measured in a two-electrode configuration. The open circuit voltages in the dark were ~ -0.64 and -0.75 V for the *p*-GaInP₂(Pt) and *p*-GaInP₂(Pt)/TJ/GaAs electrodes, respectively. The dark reduction current was small (in microampere range) for both electrodes. Under illumination, the *p*-GaInP₂(Pt) electrode started to generate hydrogen at a voltage 500 mV negative of 0 V bias, indicating that additional external voltage was needed for this semiconductor to split water. Under illumination, the *p*-GaInP₂(Pt)/TJ/GaAs electrode showed an open-circuit voltage of ~ 0.55 V, indicating the extra photovoltage generated by the GaAs cell. Evolution of H₂ started immediately, 400 mV positive of a short circuit. The photocurrent density reached a limiting value of 120 mA/cm² at ~ 0.15 V and remained almost constant with increasing bias. Copious amounts of gas bubbles could be observed at the semiconductor surface. Because these gas bubbles can grow to sufficient size to act as miniature lenses, causing pitting of the semiconductor electrode, 0.01 M of the surfactant Triton X-100 was added to the solution to promote the formation of smaller bubbles that left the sample surface more rapidly. The lower saturated photocurrent for the *p*-GaInP₂(Pt)/TJ/GaAs electrode as compared to the *p*-GaInP₂ electrode is taken to indicate that the *p/n* GaAs bottom cell is the current-limiting junction.

The photocurrent time profile for the *p*-GaInP₂(Pt)/TJ/GaAs electrode at short-circuit condition is shown in Fig. 3. The current density decreased slightly for about 300 s but then stabilized at about 120 mA/cm² and remained constant throughout the first part of the experiment. The inset in Fig. 3 shows the long-term current stability of the *p*-GaInP₂(Pt)/TJ/GaAs electrode. After 20 hours, the initial current density of 120 mA/cm² decreased to 105 mA/cm². Gas bubbles continued to be evolved from the entire surface. Visual inspection of the electrode surface after the experiment revealed some localized damage of the sample along the upper edge of the epoxy coating, where gas bubbles collect and are held by the "lip" of the epoxy. The remaining portion of the sample appeared undamaged. Because these experiments were done with the electrode in a vertical position, a more solar-like slanted position (not possible with our current configuration) would reduce or eliminate the accumulation of bubbles at this edge.

The products of photoelectrolysis were collected and analyzed with a mass spectrometer. Within our experimental error, the ratio was 2:1 H₂:O₂ as expected (23). The efficiency of H₂ production was calculated with the following equation: efficiency = (power out)/(power in). The input power is the incident light intensity of 1190 mW/cm². For the output power, assuming 100% photocurrent electrolysis efficiency, the H₂ production photocurrent of 120 mA/cm² is multiplied by 1.23 V, which is the ideal fuel cell limit at 25°C (the lower heating value of hydrogen). Calculated by this method, the H₂ production efficiency of our system is 12.4% (24).

Gerischer (2) has calculated for a two-layer semiconductor system (a tandem cell) that the maximum efficiency of photoelectrochemical water splitting would be 24%. Bolton *et al.* (16) estimated 16% as a maximum realizable chemical conversion efficiency for a tandem system of this type (a D4 scheme in his nomenclature). Weber and Dignam (25, 26) calculated that for different tandem cell configurations, the maximum water-splitting efficiency would fall between 10 and 18%. Their efficiency analysis took into account various solid-state and electrochemical losses. Our results are consistent with these calculations.

The key to making this system work appears to be the requirement that the bottom cell be the limiting electron provider. Because these tandem systems operate by requiring two photons (one per junction) to produce one electron in the external circuit, great care is taken in the solid-state systems to match the photon absorption characteristics so that equal numbers of

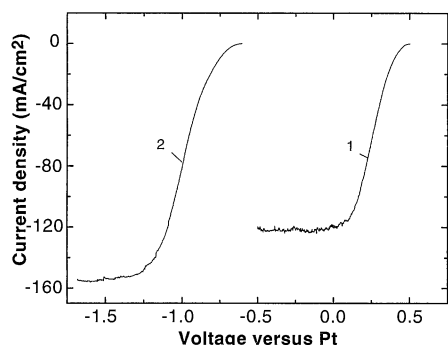


Fig. 2 (left). Current-voltage characteristics for *p*-GaInP₂(Pt)/TJ/GaAs (curve 1) and *p*-GaInP₂ (curve 2) electrodes in 3 M H₂SO₄ under white light illumination.

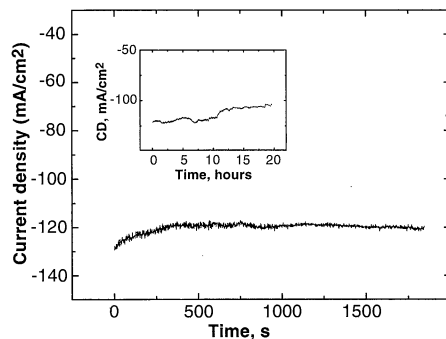


Fig. 3 (right). Photocurrent time profile at the *p*-GaInP₂(Pt)/TJ/GaAs electrode with 0.01 M Triton X-100 under tungsten-halogen white light illumination.

photocarriers are generated in the top and bottom cells. However, when the photocurrent-matched configuration is placed in an aqueous environment, the system either produces no current in the external circuit or decomposes (27). A thicker, top *p*-type layer and the resultant mismatch of electron-hole formation in the two-junction region appear to be the key for proper operation.

REFERENCES AND NOTES

1. A. J. Bard and M. A. Fox, *Acc. Chem. Res.* **28**, 141 (1995).
2. H. Gerischer, in *Topics in Applied Physics*, vol. 31, Solar Energy Conversion, B. O. Seraphin, Ed. (Springer-Verlag, Berlin, 1979), pp. 115–172.
3. The ability of a semiconductor electrode to drive the electrochemical reaction of interest is determined by its band gap (the energy separation between the valence and conduction band edges) and the position of the valence and conduction band edges relative to the vacuum level (or other reference electrode). In contrast to metal electrodes, semiconductor electrodes in contact with liquid electrolytes have fixed energies where the charge carriers enter the solution. This fixed energy is given by the energetic position of the semiconductor's valence and conduction bands at the surface (where these bands terminate at the semiconductor/electrolyte interface). The energetic position of these band edges is determined by the chemistry of the semiconductor/electrolyte interface, which is controlled by the composition of the semiconductor, the nature of the surface, and the electrolyte composition. So even though a semiconductor electrode may generate sufficient energy to effect an electrochemical reaction, the energetic position of the band edges may prevent it from doing so. For spontaneous water splitting, the oxygen and hydrogen reactions must lie between the valence and conduction band edges, and this is almost never the case.
4. G. E. Shakhnazaryan *et al.*, *Russ. J. Electrochem.* **30**, 610 (1994).
5. E. Aharon-Shalom and A. Heller, *J. Electrochem. Soc.* **129**, 2865 (1982).
6. A. Heller, *Science* **223**, 1141 (1984).
7. S. Kocha, J. Turner, A. J. Nozik, *J. Electroanal. Chem.* **367**, 27 (1991).
8. S. Kocha and J. A. Turner, *J. Electrochem. Soc.* **142**, 2625 (1995).
9. H. Yoneyama, H. Sakamoto, H. Tumura, *Electrochem. Acta* **20**, 341 (1975).
10. A. J. Nozik, *Appl. Phys. Lett.* **29**, 150 (1976).
11. R. C. Kainthla, B. Zelenay, J. O'M. Bockris, *J. Electrochem. Soc.* **134**, 841 (1987).
12. Y. Sakai *et al.*, *Can. J. Chem.* **66**, 1853 (1988).
13. G. Lin *et al.*, *Appl. Phys. Lett.* **55**, 386 (1989).
14. J. Augustynski, G. Calzaferri, J. Courvoisier, M. Graetzel, in *Proceedings of the 11th World Hydrogen Energy Conference*, T. N. Veziroglu, C.-J. Winter, J. P. Baselt, G. Kreysa, Eds. (DECHEMA, Frankfurt, Germany, 1996), pp. 2378–2387.
15. K. A. Bertness *et al.*, *App. Phys. Lett.* **65**, 989 (1994).
16. J. R. Bolton *et al.*, *Nature* **316**, 495 (1985).
17. S. R. Kurtz *et al.*, *J. Appl. Phys.* **68**, 1890 (1990).
18. K. A. Bertness *et al.*, in *AIP Conference Proceedings No. 306*, R. Noufi and H. Ullal, Eds. (American Institute of Physics, New York, 1994), p. 100.
19. O. Khaselev and J. A. Turner, in preparation.
20. For electrochemical measurements, the wafers were cleaved into samples ~ 0.2 cm² in area. The samples with gold ohmic contacts were mounted on a Teflon-covered screw electrode with silver epoxy and heated to 80°C for 1 hour. The electrical contact was insulated from the electrolyte by an epoxy coating that also covered the samples' edges. A conventional two-electrode configuration was used with a platinum gauze or foil counter-electrode coated with ruthenium metal. Photoelectrochemical characteristics were measured with an EG&G 263A potentiostat. The electrolyte, 3 M H₂SO₄, was freshly prepared from deionized water having resistivity of 18 megohm/cm. All solutions were made of analytical-grade reagents. Before electrochemical measurements, the samples were etched in 1:20:1 HCl:CH₃COOH:H₂O₂ solution. A single-compartment cell was used. Although the electrodes were spatially separated, no attempt was made to separate the products of the anode and cathode reactions.
21. To reduce the overvoltage losses associated with the noncatalytic surface of the semiconductor, a thin layer of platinum catalyst was electrochemically deposited on the surface of the semiconductor electrodes from a 20 mM H₂PtCl₆ solution. Photoassisted galvanostatic deposition was performed at a cathodic current density of 1 mA/cm², with a platinum quantity corresponding to a charge of 10 mC/cm². A recent publication (28) has shown that the platinum not only acts as a catalyst for hydrogen evolution but also drastically reduces the corrosion reaction of a similar III-V compound, indium phosphide. We would expect that platinum would offer a comparable corrosion-inhibiting mechanism here.
22. We used concentrated light for two reasons: (i) The photocurrent and the amount of gases produced are higher and therefore easier to quantify, and (ii) because of their cost, the major terrestrial application of the solid-state analog of these tandem cells is in concentrator systems (>100 suns). Therefore, any real application using the present solid-state design for photoelectrolysis would also use concentrated light. However, the PEC systems will probably be limited to less than 100 suns, because that would give rise to a current of about 1A/cm², a practical limit for electrolysis. The evolution of gas bubbles on the illuminated surface is also an issue, as these bubbles will scatter light, reducing the efficiency. Given this limitation as well as problems regarding the amount of catalyst and system design issues, a more realistic limit as to the amount of light concentration that can be used for photoelectrolysis is in the range of 10 to 20 suns.
23. The gas products of the photoelectrolysis were analyzed with a UTI-100C mass spectrometer. A sealed cell was used, connected directly to the high-vacuum chamber of the mass spectrometer via a gas inlet system. Before being sealed, the cell was purged for several minutes with nitrogen to remove any oxygen. The cell was then sealed, and the photoelectrolysis reaction was run for several hours. The external current was monitored with an ammeter. Periodically, the gas mixture from the upper part of the cell was sampled by the mass spectrometer system. The same cell was used and the same experimental technique was repeated with the use of two platinum electrodes at the same external current. Within experimental error ($\sim \pm 20\%$), the results were the same, indicating stoichiometric water splitting.
24. For 100% electrolysis efficiency, this calculation is identical to Bolton's calculation of efficiency (29). For the size of these samples and the amount of hydrogen and oxygen being generated, a calculation using external current flow is far more accurate.
25. M. F. Weber and M. J. Dignam, *Int. J. Hydrogen Energy* **11**, 225 (1986).
26. ———, *J. Electrochem. Soc.* **131**, 1258 (1984).
27. S. Kocha, D. Montgomery, M. Peterson, J. A. Turner, *Sol. Energy Mater. Sol. Cells*, in press.
28. P. Bogdanoff, P. Friebe, N. Alonso-Vante, *J. Electrochem. Soc.* **145**, 576 (1998).
29. J. R. Bolton, *Solar Energy* **57**, 37 (1996).
30. We thank S. Kurtz and J. Olson for the tandem cell samples and A. Dillon for help with the mass spectrometer measurements. This work was supported by the Hydrogen Program of the U.S. Department of Energy.

18 November 1997; accepted 23 February 1998

Gastrointestinal Tract as a Major Site of CD4⁺ T Cell Depletion and Viral Replication in SIV Infection

Ronald S. Veazey, MaryAnn DeMaria, Laura V. Chalifoux, Daniel E. Shvetz, Douglas R. Pauley, Heather L. Knight, Michael Rosenzweig, R. Paul Johnson, Ronald C. Desrosiers, Andrew A. Lackner*

Human and simian immunodeficiency virus (HIV and SIV) replicate optimally in activated memory CD4⁺ T cells, a cell type that is abundant in the intestine. SIV infection of rhesus monkeys resulted in profound and selective depletion of CD4⁺ T cells in the intestine within days of infection, before any such changes in peripheral lymphoid tissues. The loss of CD4⁺ T cells in the intestine occurred coincident with productive infection of large numbers of mononuclear cells at this site. The intestine appears to be a major target for SIV replication and the major site of CD4⁺ T cell loss in early SIV infection.

It is now thought that ongoing HIV replication results in a continual loss of CD4⁺ T lymphocytes that is nearly balanced by the production of new CD4⁺ T lymphocytes (1). This model explains some of the puzzles of HIV infection, but the events that occur in the initial stage of infection remain largely unexplored. Although it is clear that HIV targets lymphoid tissue, nearly all studies in this area have focused on peripheral blood and lymph nodes. These studies overlook the

fact that the gastrointestinal tract contains most of the lymphoid tissue in the body (2, 3). Furthermore, it is likely that the behavior of HIV in the unique immunologic environment of the intestinal mucosa differs from that observed in the periphery.

The gut-associated lymphoid tissue (GALT) consists of organized lymphoid tissue (Peyer's patches and solitary lymphoid follicles) as well as large numbers of activated memory T lymphocytes diffusely dis-